LA-UR-13-26931
Approved for public release; distribution is unlimited.

Title: IMPACT - Integrated Modeling of Perturbations in Atmospheres for Conjunction Tracking

Author(s): Koller, Josef
Brennan, Sean M.
Godinez Vazquez, Humberto C.
Higdon, David M.
Klimenko, Alexei V.
Larsen, Brian A.
Lawrence, Earl C.
Linares, Richard
Mehta, Piyush
Palmer, David
Shoemaker, Michael A.
Thompson, David C.
Walker, Andrew C.
Wohlberg, Brendt E.
Jah, Moriba
Sutton, Eric
Kelecy, Thomas
Ridley, Aaron
McLaughlin, Craig

Intended for: AMOS Conference, 2013-09-10/2013-09-13 (Wailea, Maui, Hawaii, United States)
Report
Web

Issued: 2013-09-05

IMPACT – INTEGRATED MODELING OF PERTURBATIONS IN ATMOSPHERES FOR CONJUNCTION TRACKING

Josef Koller[1]
Sean Brennan
Humberto Godinez
David Higdon
Alexei Klimenko
Brian Larsen
Earl Lawrence
Richard Linares
Piyush Mehta
David M. Palmer
Michael Shoemaker
David Thompson
Andrew Walker
Brendt Wohlberg
Los Alamos National Laboratory

Moriba Jah, Eric Sutton
Air Force Research Laboratory

Thomas Kelecy
The Boeing Company

Aaron Ridley
University of Michigan

Craig McLaughlin
University of Kansas

ABSTRACT

The United States relies heavily on its space infrastructure for a vast number of applications, including communication, navigation, banking, national security, and research. However, NASA predicts that between now and 2030 orbital collisions will become increasingly frequent and could reach a runaway environment. This devastating scenario, also known as the Kessler Syndrome, has the potential to eventually destroy our assets in near-Earth space and result in a debris cloud that could make space itself inaccessible. Preventing the Kessler Syndrome requires, in addition to an object removal technique, a groundbreaking new orbital dynamics framework that combines a comprehensive physics-based model of atmospheric drag with an accurate uncertainty quantification of orbital predictions. The IMPACT project (Integrated Modeling of Perturbations in Atmospheres for Conjunction Tracking), funded with over $5 Million by the Los Alamos Laboratory Directed Research and Development office, has the goal to develop such an integrated system of atmospheric drag modeling, orbit propagation, and conjunction analysis with detailed uncertainty quantification to address the space debris and collision avoidance problem. We discuss the components and capabilities of the IMPACT framework and show a short demonstration of modeling interface and resulting 3D visualizations.

[1] Project PI: Josef Koller, jkoller@lan.gov

1. INTRODUCTION

The IMPACT (Figure 1) project, funded by an internal research and development process at Los Alamos National Laboratory (LANL), has the goal to develop an integrated modeling system for addressing current needs in space debris and conjunction analysis for resident space objects (RSO) in low-Earth orbit. Now with almost three years into the project, we have developed an integrated solution combining physics-based density modeling of the upper atmosphere between 120-700 km altitude, satellite drag forecasting for quiet and disturbed geomagnetic conditions, and conjunction analysis with non-Gaussian uncertainty quantification. We are employing several novel approaches including

- a Raven-class observational facility for ground-based observations of space objects
- physics-based density modeling and data assimilation for integrating density measurements with model forecasts similar to terrestrial weather prediction
- drag coefficient modeling with Test Particle and Direct Simulation Monte Carlo methods to accurately account for changes in density, chemical composition, temperature and their effect on the drag coefficient and orbit propagation during geomagnetic storms
- atmospheric density reconstruction using Satellite Orbit Tomography based on X-ray Computed Tomography from the medical imaging field
- collision statistics and uncertainty quantification using full Monte Carlo sampling and importance sampling for collisional probabilities and allowing for non-Gaussian probability distributions
- machine learning approach to enable a coupling between solar drivers and the upper atmosphere resulting in tremendous computational efficiency while preserving modeling accuracy

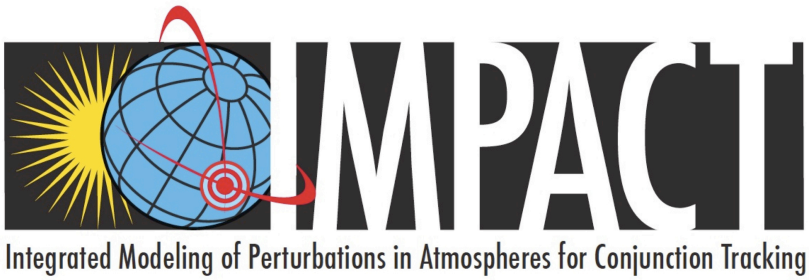

Figure 1 IMPACT logo

In the following subsection, we will describe in details some of the technological developments as part of the IMPACT project.

2. GROUND BASED OBSERVATIONS

LANL is using a Raven-class telescope (0.35 m aperture C14 on a Paramount ME mount) to track satellites. This observational facility is located at 2650 m altitude under dark skies about an hour from Los Alamos, NM. We typically take several nights of observation around each New Moon, weather and wildfire permitting. This provides both good metric accuracy for orbit determination and lightcurves for object characterization. The objects we observe for IMPACT are primarily:

a) Satellites with accurately known orbits, which we use to characterize the accuracy of our metric determinations. These satellites include the GPS and WAAS constellations, geodesy satellites, and satellites carrying on-board GPS receivers.

b) Cubesats, many of which are similar in terms of mass, volume, shape, and surface materials and hence are good test particles for looking at atmosphere-induced variation in drag. We also observe other LEO satellites that have size/shape/mass information available.

c) Objects in highly eccentric orbits that dip into the atmosphere at perigee. The drag perturbation over an orbit for one of these objects is dominated by the atmosphere at the geographic location and altitude of the perigee pass. Rocket bodies in GTO are numerous and particularly useful, since they tend have known physical characteristics. We produce light-curves from our observations in order to derive the spin-states of the objects, which affect the average frontal area around the time of perigee.

We have also observed debris from satellite collisions and the Breeze-M explosion. These observations include over 300 different RSOs, including 26 GPS satellites and 76 rocket bodies.

3. PHYSICS-BASED DENSITY FORECAST MODELING

A key element in improving satellite orbital predictions is the correct specification of the ionosphere-thermosphere environment, given that atmospheric density exerts significant drag over satellites. There are a number of models that can estimate the composition and density of the ionosphere-thermosphere, from empirical models to physics based models. Empirical models, such as the Mass Spectrometer and Incoherent Scatter (MSIS) [1] model, can provide an accurate estimation of current or past ionosphere-thermosphere density, based on a number of observations. Unfortunately, these types of models do not have predictive capabilities, that is, they provide a good nowcast but are often not suitable for a forecast. The IMPACT project uses a physics-based model, which has the potential to estimate a forecast of the ionosphere-thermosphere since they include the relevant physical behavior of the system. In particular, the project uses the Global Ionosphere-Thermosphere Model (GITM) [2] but the IMPACT framework is in able to switch between different models for comparative studies.

3.1 Ionosphere-Thermosphere Models and Assimilation Method

GITM is a physics-based three-dimensional model that solves the full Navier-Stokes equations for density, velocity, and temperature for a number of neutral and charged components. To account for solar activity, GITM uses at the moment the F10.7 solar flux, hemispheric power index (HPI) (which is derived from the 3-hour Kp), interplanetary magnetic field (IMF) data and solar wind velocity. GITM inherently allows for non-hydrostatic solutions to develop which allows for realistic dynamics in the auroral zones [2]. As with many of the physics-based models, GITM includes a number of assumptions and physical representation of the ionosphere-thermosphere that might not be accurate and introduce errors into the estimation of the density. This severely affects the quality of a density forecast.

In order to improve the predictability of GITM, and provide a good forecast of the ionosphere-thermosphere, we implement a data assimilation system based on the ensemble Kalman filter (EnKF) [3,4]. The EnKF uses an ensemble of model simulations to approximate the probability distribution of the model, as well as the covariance matrix. The main advantages of the EnKF are the ease of implementation and the computational efficiency for non-linear models. In particular we use the localized ensemble transform Kalman filter (LETKF) [5], which is a localized version of the EnKF. The LETKF assimilates by local volume centered at each grid-point variable, where the area of the local volume depends on model dynamics and assumptions of correlations between model variables. Given the local nature of the LETKF, the algorithm is highly parallel since all grid-point variables can be assimilated simultaneously.

3.2 Assimilation of Derived Density Fields

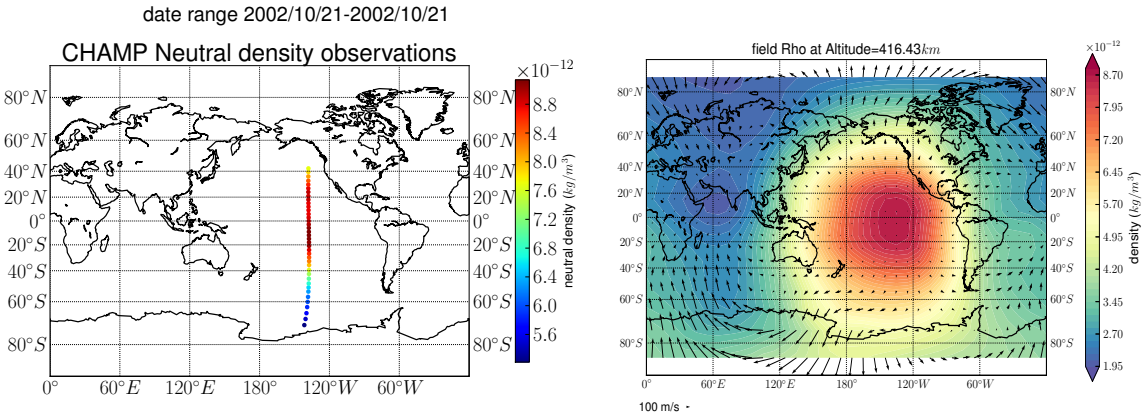

Figure 2: Example of data assimilation: (left) CHAMP observations over a 30 minute assimilation window; (right) assimilated state after combining CHAMP observations with GITM forecast.

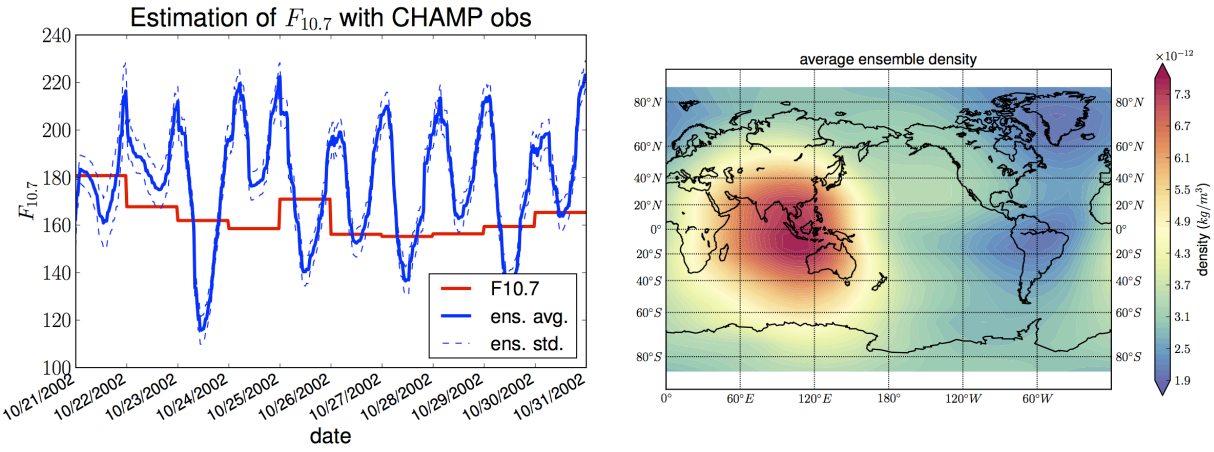

Figure 3: Left plot: daily averaged measured F10.7 (red line), ensemble average F10.7 from the assimilation of CHAMP neutral density observations (blue line) and ensemble standard deviation for F10.7 (blue dashed line). The oscillations in the estimated F10.7 seems to follow the day-night change seen by the CHAMP satellite. Right plot: ensemble average density field for October 21 2002 at 0800 hours UTC.

To enhance the density estimation of GITM with data assimilation, we use derived density observations from the CHAllenging Minisatellite Payload (CHAMP) [6,7] and Gravity Recovery and Climate Experiment (GRACE) [8] missions. Both mission satellites have GPS and accelerometer data that are processed to estimate a neutral density field [9]. Figure 2 shows an example of assimilating a 30 minute observational window into the GITM forecast. Given the scarcity of the data, it is challenging to constrain the whole model field. To address this issue, the assimilation is used to estimate both model variables and key model parameters that influence the global evolution of the model. To select the most relevant model parameter(s), a sensitivity study was performed a reveled that a key parameter is F10.7 index. This result is consistent with the physical representation of the F10.7 index within the model, since it is being used as a proxy for solar activity. The F10.7 index is not strictly an independent input parameter for the model, since it's a measured index. Therefore, the assimilation will "calibrate" this index by adding a correction provided by the data assimilation. That is, the assimilation estimates $\delta F_{10.7}$ for the model input index in the following way,

$$F^{m}_{10.7} = F_{10.7} + \delta F_{10.7} \qquad (1)$$

where $F^{m}_{10.7}$ is the model index used by GITM, and $F_{10.7}$ is the observed index. In this formulation, the correction to F10.7 is actually taking into account model bias and trying to correct it using data assimilation.

Figure 3 shows the daily averaged measured F10.7 value (red line), the ensemble average of the estimated F10.7 (blue line) using data assimilation with CHAMP data, as well as the ensemble standard deviation of F10.7. All index values are valid for October 21-31 2002. The estimated F10.7 value (blue line) is oscillating in accordance with the day-night position of the CHAMP satellite, indicating that the assimilation is correcting an overestimation/underestimation, suffered by the GITM model, through the F10.7 index. The left plot shows the ensemble average neutral density estimation for October 21 2002 at 0800 hours UTC.
The assimilation results indicate that using data assimilation can reduce the forecast error of the model. Furthermore, the model bias can be corrected through the calibration of key model parameters through data assimilation. Other key parameters that influence other fields and properties of the mode, such as temperature, composition, etc., will be explored and included for calibration in the data assimilation. Initial condition and boundary conditions are also a concern for the model simulation, and will be addressed in the assimilation scheme as well.

4. DRAG COEFFICIENT MODELING

Drag is the largest source of uncertainty in the orbital trajectories of satellites in low Earth orbit (LEO). The acceleration on a satellite due to drag, $\vec{a}_D$, is defined by [10]

$$\vec{a}_D = \frac{1}{2}\rho C_D \frac{A}{m} v_{rel}^2 \frac{\vec{v}_{rel}}{\left|\vec{v}_{rel}\right|}$$

where ρ is the local atmospheric mass density, C_D is the satellite drag coefficient, A is the projected area of the satellite normal to the velocity vector, m is the satellite mass, and v_{rel} is the relative velocity between the satellite and the co-rotating atmosphere. For artificial satellites, the primary source of drag acceleration uncertainty stem from inadequate knowledge of ρ and C_D.

Atmospheric mass densities are often inferred from the orbital decay of satellites by using fixed or fitted drag coefficients [11,12]; however, the use of such drag coefficients introduces biases into the inferred mass densities [1]. These biases can be partially removed by using physical drag coefficients computed based on the momentum exchange between atmospheric particles and the satellite surface. The vast majority of LEO satellites orbit in free molecular flow where intermolecular collisions between atmospheric particles can be neglected. In such conditions, the drag coefficients for satellites with simple convex geometries have closed-form solutions [13–15]. A numerical method, such as Test Particle Monte Carlo (TPMC), is required to accurately calculate drag coefficients for satellites with complicated concave geometries. At lower altitudes, where the free molecular flow assumption breaks down, a rarefied gas dynamic technique that accounts for intermolecular collisions, such as Direct Simulation Monte Carlo (DSMC), is required [16].

Physical drag coefficients are dependent on a variety of atmospheric and satellite properties, including: atmospheric translational temperature, satellite surface temperature, relative velocity between the satellite and the co-rotating atmosphere, atmospheric composition, satellite surface composition, and, most importantly, the gas-surface interaction (GSI) [13,15]. The GSI is generally controlled by one or more momentum or energy accommodation coefficients, depending on the GSI model. One of the simplest GSI models, Maxwell's model, is not dependent on accommodation coefficients. Instead, Maxwell's model splits the population of reflected particles into a fraction, ϵ, that is reflected specularly, while the remaining portion, 1-ϵ, are diffusely reflected. Recently, we have recently shown in [17] that Maxwell's model is incapable of matching fitted drag coefficients as a function of altitude. Two more sophisticated GSI models are diffuse reflection with incomplete accommodation (DRIA) [18] and the Cercignani-Lampis-Lord (CLL) model [19]. The DRIA model has been applied in satellite drag coefficient modeling for nearly 50 years; however, the CLL model was only recently applied to satellite drag coefficient modeling for first time by our group [17].

We have developed closed-form solutions [17] for simple convex geometries such as a sphere and flat plate for use with the CLL GSI model. Closed-form solutions were developed by fitting analytic expressions (modified from the original Schaaf and Chambre [13] solutions) to DSMC simulations with NASA's DAC [20] that were sampled from the global parameter space using Latin Hypercube sampling. These CLL closed-form solutions fit the DAC simulations within ~0.5% of the global parameter space.

Decades of work by Moe et al. [21–25] has shown that satellite surfaces are likely covered by varying levels of atomic oxygen. The atomic oxygen adsorbate changes the nature of the GSI, specifically, the effective energy accommodation coefficient, α in the DRIA model, when compared to particles interacting directly with a clean spacecraft surface. Pilinski et al. [26] was the first to fit the variation of α as a function of altitude with a Langmuir isotherm dependent on the partial pressure of atomic oxygen, P_O; however, their original model had several deficiencies, including α going to zero as P_O goes zero. Walker et al. [17] and Pilinski et al. [27] have improved upon this deficiency by computing α as a weighted sum of unit accommodation (α_{ads} - *1*)due to the adsorbate covered surface) and the energy accommodation coefficient of the clean satellite surface, α_{ads}, based on Goodman's formula [28]

$$\alpha = (1-\theta)\alpha_{srf} + \theta\alpha_{ads}$$

$$\alpha_{srf} = \frac{2.4\mu}{(1+\mu)^2}$$

We compared CLL and DRIA GSI models [17] while including the effects of atomic oxygen adsorption and found that both models can match fitted drag coefficients [29] equally well below ~500 km altitude. They also found larger (greater than ~20%) variations in the drag coefficients of simple geometries between solar minimum and solar

maximum, confirming previous results from Moe et al. [22]. We investigated also in [17] the differences in drag coefficients computed using NRLMSISE-00 [1] and Global Ionosphere-Thermosphere Model (GITM) [2] atmospheric properties. At solar maximum, minor drag coefficient discrepancies of ~3% were found; however, much larger differences (up to ~11%) were found during solar minimum.

More recently, we developed a response surface model (RSM) technique [30] for drag coefficient modeling. The method was validated for a sphere and then extended to the more realistic case of the GRACE satellite. Comparison of the original TPMC training simulations and the RSM predictions show errors of ~0.25% for the sphere and ~0.7% for GRACE. We compared in [31] Langmuir, Temkin, and Freundlich adsorption models and showed that the Temkin and Freundlich models match fitted drag coefficients better and both low and high altitudes. Furthermore, both adsorption models alleviate some of the physical deficiencies present in the Langmuir model, such as constant adsorption energy and monolayer adsorption.

5. ATMOSPHERIC DENSITY RECONSTRUCTION

The ground-based tracking observations are used to estimate the orbital state and drag ballistic coefficient of a number of satellites. By analyzing the change in the satellites' orbits over time, one can estimate the atmospheric neutral density, in the form of corrections to an assumed density model. This approach is often called a Dynamic Calibration of the Atmosphere (DCA) in the literature [10]. This "nowcast" density estimate can then be fed into the data assimilation described above to provide better physics-based density forecasts.

We have developed a new DCA method called Satellite Orbit Tomography, which was originally inspired by X-ray computed tomography. Here, rather than using the decay in X-ray intensity, we use the decay in orbital specific mechanical energy (ξ). Shoemaker et al [32] describes the mathematical formulation, and Shoemaker et al [33] gives simulation results of an operationally realistic scenario. The method is outlined as follows:

- Identify a set of target satellites for tracking, nominally those that are inactive (e.g. debris, rocket bodies). Track each target over a span of time (>days) to build up estimates of the position, velocity, and drag ballistic coefficient (β). In the simulations considered to date, we have used a Constrained Admissible Region Multiple Hypothesis Filter (CAR-MHF) [34–36] to estimate these states based on measured angles and angle-rates.
- Remove bias in the estimated β introduced by global errors in the assumed density model used in the CAR-MHF. This is done by including at least some tracking targets that have fairly well-modeled β, and comparing their modeled β with that estimated by the CAR-MHF. This approach also leverages the drag coefficient modeling described above: given the published information on a satellite's shape and mass, we are able to sufficiently model β.
- Using a given satellite's estimated position and velocity at one time (t_1), and then again at a later time (t_2), calculate the decay in ξ using the osculating orbit states at those times. The time span $\Delta t = t_2 - t_1$ should be long enough to observe the decay signal above the measurement noise, yet short enough to recover some time-resolved information in the density model. Our simulations have used Δt of 48 hours, but a lower limit of 24 hours is feasible given the expected accuracy of our ground-based tracking system and the likely revisit rate (~1 to 2 passes per night) for our mostly LEO targets.
- Using the measured decay in ξ from the set of targets, solve for a spatially-resolved scalar correction (s) to the assumed density model. The correction factor s is defined in a grid; we have used grids spanning 300 to 500 km altitude, with 100 km altitude spacing and 20 deg spacing in latitude and longitude. In general, the problem is underdetermined (there are more grid elements than target satellites) and ill-posed (most satellites do not pass through each grid element). Thus, we use Tikhonov regularization to stabilize the solution, with a spatial smoothness constraint on the solved-for s field.

Our most recent simulations use actual resident space objects from the publically available catalog, and assume a single ground site at Fenton Hill, NM. Using only 40 targets and having suitable visibilities from this single ground site, we are able to reconstruct the time-averaged, yet spatially resolved, density field over 48 hours to within approximately 10%. These results also assume reasonable orbit estimation errors, and that each satellite's assumed ballistic coefficient β will have zero-mean error with 1-σ standard deviation of 10%. The satellite orbit tomography approach has some practical advantages over typical weighted least-squares approaches, such as allowing easy density model specification i.e. not requiring Jacobian matrices that describe the sensitivity of the density model dynamics to the states.

6. MACHINE LEARNING FOR FAST DENSITY FORECASTING

Given the significant computational expense of a full physics-based simulation of the spatial variation of the atmospheric density profile, there is a need for a rapidly computable model approximating this profile. Our goal is to apply machine-learning methods to construct such a model, enabling estimation of the density profile based on current measurements of physical parameters such as solar activity and terrestrial magnetic field. Our initial attempts to learn a model based on historical point-measurements of atmospheric density from instrumented satellites (e.g. CHAMP and GRACE) showed that the spatial sampling density of available data is entirely inadequate for such a task. Our current approach, therefore, is to construct a computationally cheap surrogate model learned from simulations produced by the GITM code; this work is still in progress. Our initial task has been the construction of a low-dimensional parameterization of the density profile; given the difficulty of directly estimating a full, high-dimensional representation of the profile, a regression model will be constructed to estimate the low-dimensional parameterization from the available physical measurements. While spherical harmonics are a very widely used basis on which to represent these profiles, we are currently investigating the use of a basis derived from our training data (i.e. a set of GITM simulations) via Principal Component Analysis (PCA).

7. UNCERTAINTY QUANTIFICATION

Our goal is to compute collision probabilities that account for uncertainty at each stage of our modeling procedure. To be accurate, a collision probability must necessarily incorporate uncertainty from observations, density modeling and forecasting, drag estimation, and other sources. In order to combine uncertainty across these sources, we favor Monte Carlo-based methods.

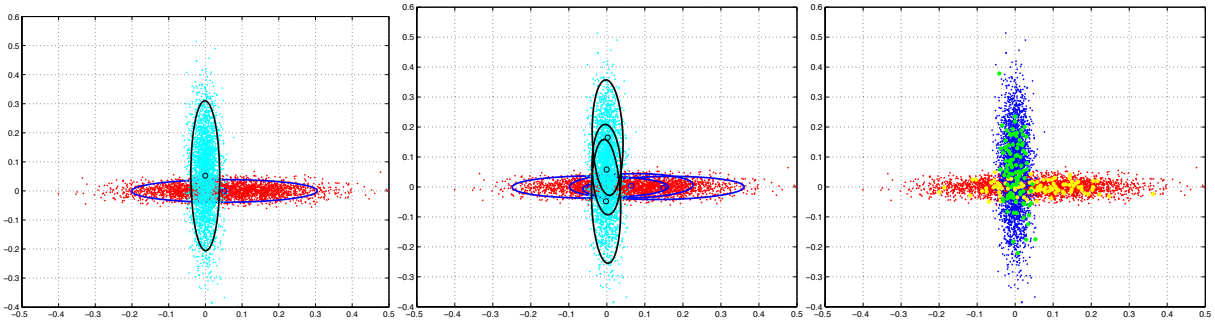

Figure 4: (left) Gaussian approximations to Monte Carlo samples for a simulated example. (middle) Mixture of Gaussian approximation to Monte Carlo sample from a simulated example. (right) The yellow and green points show 100 importance sampled points using the two-stage procedure. This small sample produced a very accurate estimate of the probability when compared to a brute force simulation of 9,000,000 pairs.

The recent FORTE/Meteor close approach on 22 June 2013 provided an opportunity to test a basic Monte Carlo strategy. First, we sampled ten GITM densities from the distribution of possible densities. Next, we sampled 100 satellite state vectors from the distribution induced by observations of the two satellites made before the close approach. These state vector samples were randomly paired with a sampled GITM density and the pair was propagated to close approach. At the time of close approach, we approximated the distribution of the positions with a simple Gaussian and used this to calculate the probability of collision. This method required relatively few simulations and incorporated two important sources of uncertainty. More uncertainty sources could be incorporated very easily (we calculated a best fit drag coefficient, but weren't able to compute uncertainty at the time), although this would likely require a larger set of simulations. Figure 4 (left) shows a fit based on a similar simulated close approach.

A simple extension of the previous method is the use of a mixture of Gaussian model for the positions at close approach. This collision probability would be more accurate since the mixture model would be a better representation of the final position uncertainty. The calculation is a straightforward extension of the single Gaussian case. One drawback is that this method would require a larger set of simulations in order to accurately estimate the mixture model. Figure 4 (middle) shows the mixture of Gaussian fit to the same simulation as the figure on the left. Notice that this fit is better at capturing the tails and the overly dense central region.

We are also working on an *importance sampling* methodology for computing collision probabilities with reduced simulation costs. Importance sampling is a Monte Carlo method that draws a biased sample that is weighted to produce the correct expectations. Particularly in the case of small probabilities, this technique can be used to reduce the variance of an estimate, and therefore the number of samples required. We developed a two-stage procedure. In the first stage a raw Monte Carlo sample is drawn from all of the uncertainty sources. The results of this stage are analyzed to find regions of the original distribution that produce close approaches and the second stage samples directly from these regions. Figure 4 (right) shows the results of the methodology applied to the simulations shown in figures on the left and middle. The second stage used 100 simulations to accurately estimate the collision probability when compared with a brute force simulation.

8. MODEL INTEGRATION AND VISUALIZATIONS

In order to coherently integrate these diverse models (Figure 5), plus alternative models to facilitate comparisons of model techniques and implementations, we have developed an integration tool. For this we chose the Python language for its rapid prototyping and its multilingual extensibility. Our tool, as open-source, pure-Python package called *sysdevel* [37], handles three aspects of this multi-model synthesis:

1. unifying potentially disparate model data in a scalable and malleable way,
2. providing a service framework for plotting and visualizing data in a web browser,
3. extending the Python build system to include external library dependencies, unit testing, and automatic documentation to ease distribution of collaborators who may use differing compute environments.

The *sysdevel* build system extends the built-in Python *distutils* package to recursively build sub-packages that each build one of our models with a normal '`python setup.py build`' call. This then, for example, descends into our GITM sub-package like a recursive '`make`' call. It locates GITM's MPI and HDF5 library dependencies and the proper Fortran compiler, fetching and installing them if any are missing by utilizing CMake-style configuration files in *sysdevel*. Finally it creates a native executable for use in a cluster. Those familiar with Python will recognize that this is well beyond the normal *distutils* build process.

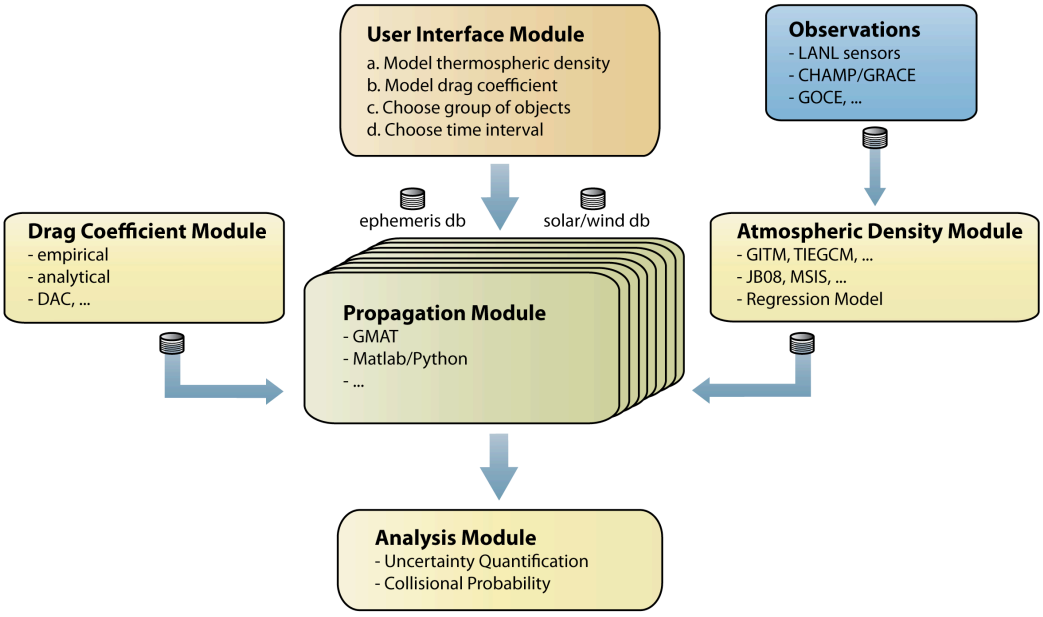

Figure 5: IMPACT Flowchart illustrating the coupling between different models for atmospheric density, drag, propagation, observations, and uncertainty quantification.

Within the IMPACT source tree, one of our sub-packages is labeled 'website' and this handles the user interface over the web. *Sysdevel* provides a Javascript and PHP framework specifically for simulation configuration and results viewing. Using a plumbing metaphor (through jsPlumb [38]), the user graphically configures the simulation processing pipeline and chooses data plots of interest. These interactive results plots are displayed as soon as data is available. To minimize computation, we store intermediate results, so data from a duplicate configuration is available immediately unless caching is overridden. Because the framework communicates with the simulation using JSON over WebSockets, we were able to extend our UI (outside of *sysdevel*) to include a 3D visualization (built with Three.js [39]) of RSO tracks around the Earth, as seen in Figure 6, with relative ease.

By far the most interesting portion of *sysdevel* is its model integration facility. With this, we build a script that acts as a server to the web interface or a direct command-line interface. *Sysdevel* combines our simulation models together using the Model-View-Controller pattern, which consists of data models (in our case, RSO objects), data controllers that manipulate those objects (our modeling processes), and data views that represent direct hooks to our plotting and visualization. Note the conflicting semantics for the word 'model' above – in the context of this well-known software pattern; we will substitute the word 'object'. These objects are the cores of our model synthesis strategy. As our development process of IMPACT iterates from 1-to-1-conjunction analysis, expanding to all-to-all RSO collision detection is challenging but the additional complexities appear feasible. Our data object abstraction supports multiple data storage backends to allow for scalability of the analysis. Currently this consists of structured Hierarchical Data Format (HDF) files, but could also utilize a relational database. As we expand to cover more and more RSOs and over wider time scales, our storage performance needs grow drastically. We are currently considering graph databases to meet that need, and our abstraction layer makes that adjustment possible.

We are not only concerned with scalability, but also malleability. We already have integrated some alternate models (such as MSIS for atmospheric density), but we want to easily include other alternatives throughout the pipeline without extensive integration work. To that end, *sysdevel* data objects are self-describing using built-in Python idioms. This feature allows us to simply alter our data object definition (by creating a new sub-class of the original Python data object) to also conform to the domain ontology of the new model, and the user is ready to go. Inside *sysdevel*, there is a great deal more complexity to map that change to the storage backend (hence our initial preference for HDF, which simplifies this mapping).

Through these features of scalable and malleable data unification, simulation pipeline configuration and data visualization, and a comprehensive build system, our *sysdevel* integration package not only serves the needs of our IMPACT project, but also provides a general tool for other multi-model simulations that would otherwise require extensive effort to tie together.

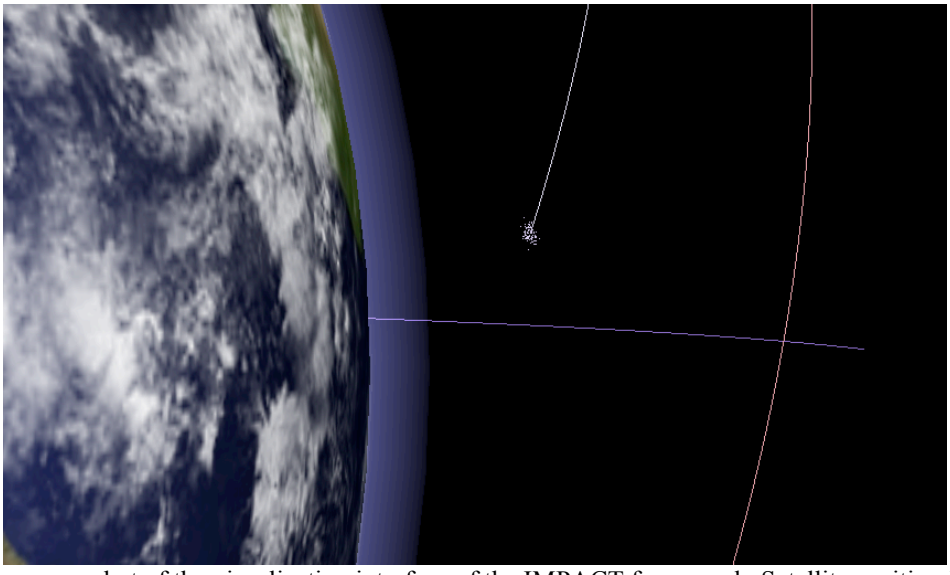

Figure 6: Screen snapshot of the visualization interface of the IMPACT framework. Satellite position is represented with a particle cloud indicating the positional uncertainty.

9. SUMMARY

The IMPACT project, funded by Los Alamos National Laboratory with internal research and development funding, has developed an open source and flexible research framework for analyzing satellite conjunctions with modern physics-based atmospheric density models, drag coefficient analysis, a new atmospheric density reconstruction method, machine learning, and system based uncertainty quantification. We presented an overview of this project including some of the novel approaches applied to satellite conjunction analysis. We welcome future collaborations using the IMPACT framework.

10. REFERNCES

[1] J.M. Picone, NRLMSISE-00 empirical model of the atmosphere: Statistical comparisons and scientific issues, Journal of Geophysical Research. 107 (2002) 1–16.

[2] A.J. Ridley, Y. Deng, G. Toth, The global ionosphere–thermosphere model, Journal of Atmospheric and Solar-Terrestrial Physics. 68 (2006) 839–864.

[3] G. Evensen, Sequential data assimilation with a nonlinear quasi-geostrophic model using Monte Carlo methods to forecast error statistics, Journal of Geophysical Research. 99 (1994) 10143–10162.

[4] G. Evensen, The Ensemble Kalman Filter: theoretical formulation and practical implementation, Ocean Dynamics. 53 (2003) 343–367.

[5] B.R. Hunt, E.J. Kostelich, I. Szunyogh, Efficient Data Assimilation for Spatiotemporal Chaos: a Local Ensemble Transform Kalman Filter, Physica D: Nonlinear Phenomena. 230 (2007) 32.

[6] C. Reigber, G. Balmino, P. Schwintzer, R. Biancale, A. Bode, J.M. Lemoine, et al., A high-quality global gravity field model from CHAMP GPS tracking data and accelerometry (EIGEN-1S), Geophysical Research Letters. 29 (2002) 94–97.

[7] C. Reigber, CHAMP mission status, Advances in Space Research. 30 (2002) 129–134.

[8] B.D. Tapley, S. Bettadpur, M. Watkins, C. Reigber, The gravity recovery and climate experiment: Mission overview and early results, Geophysical Research Letters. 31 (2004) 1–4.

[9] E.K. Sutton, R.S. Nerem, J.M. Forbes, Density and Winds in the Thermosphere Deduced from Accelerometer Data, Journal of Spacecraft and Rockets. 44 (2007) 1210–1219.

[10] D.A. Vallado, Fundamentals of Astrodynamics and Applications (Space Technology Library), Springer, 2007.

[11] M.F. Storz, B.R. Bowman, M.J.I. Branson, S.J. Casali, W.K. Tobiska, High accuracy satellite drag model (HASDM), Advances in Space Research. 36 (2005) 2497–2505.

[12] B.R. Bowman, W.K. Tobiska, F.A. Marcos, C.Y. Huang, C.S. Lin, W.J. Burke, A New Empirical Thermospheric Density Model JB2008 Using New Solar and Geomagnetic Indices, in: AMOS Conference, Honolulu, Hawaii, 18-21 Aug 2008, 2008: pp. 18–21.

[13] S.A. Schaaf, P.L. Chambre, Flow of Rarefied Gases, in: High Speed Aerodynamics and Jet Propulsion, Princeton University Press, Princeton, NJ, 1958: pp. 1–55.

[14] R. Schamberg, A New Analytic Representation of Surface Interaction for Hyperthermal Free Molecule Flow, Rand Corp., Santa Monica, CA, 1959.

[15] L. Sentman, Free Molecule Flow Theory and Its Application to the Determination of Aerodynamic Forces, Lockheed Missile and Space Co., Sunnyvale, CA, 1961.

[16] G. Bird, Molecular Gas Dynamics and the Direct Simulation of Gas Flows, Oxford University Press, Oxford, UK, 1994.

[17] A. Walker, P. Mehta, J. Koller, A Quasi-Specular Drag Coefficient Model using the Cercignani-Lampis-Lord Gas-Surface Interaction Model, (n.d.).

[18] G. Cook, Satellite Drag Coefficients, Planet. Space Sci. (1965) 929–946.

[19] C. Cercignani, M. Lampis, Kinetic models for gas-surface interactions, Transport Theory and Statistical Physics. 1 (1971) 101–114.

[20] G.J. LeBeau, A parallel implementation of the direct simulation Monte Carlo method, Computed Methods in Applied Mechanics and Engineering. 174 (1999) 319–337.

[21] K. Moe, The Effect of Adsorption on Densities Measured by Orbiting Pressure Gauges, Planet. Space Sci. 15 (1967) 1329–1332.

[22] K. Moe, M.M. Moe, Simultaneous Analysis of Multi-Instrument Satellite Measurements of Atmospheric Density, Journal of Spacecraft and Rockets. 41 (2004) 638–650.

[23] K. Moe, M. Moe, The high-latitude thermospheric mass density anomaly: A historical review and a semi-empirical model, Journal of Atmospheric and Solar-Terrestrial Physics. 70 (2008) 794–802.

[24] K. Moe, M.M. Moe, Gas–surface interactions and satellite drag coefficients, Planetary and Space Science. 53 (2005) 793–801.

[25] K. Moe, M.M. Moe, Operational models and drag-derived density trends in the thermosphere, Space Weather. 9 (2011) 1–6.

[26] M. Pilinski, B.M. Argrow, S.E. Palo, Semiempirical Model for Satellite Energy-Accommodation Coefficients, Journal of Spacecraft and Rockets. 47 (2010) 951–956.

[27] M.D. Pilinski, B.M. Argrow, S.E. Palo, U.S.A. Force, S. Command, C. Springs, Semi-Empirical Satellite Accommodation Model for Spherical and Randomly Tumbling Objects, 50 (2013).

[28] F.O. Goodman, H.Y. Wachmann, Formula for Thermal Accommodation Coefficient, 1966.

[29] C. Pardini, K. Moe, M.M. Moe, Drag and energy accomodation coefficients during sunspot maximum, Advances in Space Research. 45 (2010) 638–650.

[30] P.M. Mehta, A. Walker, C.A. Mclaughlin, J. Koller, Comparing Physical Drag Coefficients Computed with Direct Simulation Monte Carlo Using Different Gas-Surface Interaction Models, Journal of Spacecraft and Rockets. (2013) submitted.

[31] A. Walker, Drag coefficients computed by the Direct Simulation Monte Carlo method, 2013.

[32] M.A. Shoemaker, B. Wohlberg, J. Koller, Atmospheric Density Reconstruction using Satellite Orbit Tomography, Journal of Guidance, Control, and Dynamics. (2013) submitted.

[33] M.A. Shoemaker, B. Wohlberg, J. Koller, Atmospheric Density Reconstruction Using Tomography of Satellite Orbits, Kauai, Hawaii, Feb 2013, 2013.

[34] K.J. Demars, M.K. Jah, P.W.J. Schumacher, Initial Orbit Determination using Short-Arc and Angle Rate Data, IEEE Transaction on Aerospace and Electronic Systems. 48 (2012) 2628–2637.

[35] T. Kelecy, M.A. Shoemaker, M.K. Jah, Application of the Constrained Admissible Region Multiple Hypothesis Filter to initial Orbit Determination of a Break-Up, Darmstadt, Germany, 22-25 April 2013, 2013.

[36] T. Kelecy, M.K. Jah, K.J. Demars, Application of a Multiple Hypothesis Filter to near GEO high area-to-mass ratio space object state estimation, Acta Astronautica. 81 (2012) 435–444.

[37] S. Brennan, SysDevel, Https://github.com/sean-m-brennan/pysysdevel. (2013).

[38] JsPlumb, jsPlumb, Http://jsplumbtoolkit.com. (2013).

[39] Three.JS, three.js, Http://threejs.org. (2013).